

DISCOVERING COMMON FUNCTIONAL CONNECTOMICS SIGNATURES

Xiang Li¹, Dajiang Zhu¹, Xi Jiang¹, Changfeng Jin³, Lei Guo², Lingjiang Li³, Tianming Liu¹

¹Cortical Architecture Imaging and Discovery Lab, Department of Computer Science, University of Georgia, Athens, GA; ²School of Automation, Northwestern Polytechnical University, Xian, China; ³Xiangya Hospital, Central South University, Changsha, China.

ABSTRACT

Based on the structural connectomes constructed from diffusion tensor imaging (DTI) data, we present a novel framework to discover functional connectomics signatures from resting-state fMRI (R-fMRI) data for the characterization of brain conditions. First, by applying a sliding time window approach, the brain states represented by functional connectomes were automatically divided into temporal quasi-stable segments. These quasi-stable functional connectome segments were then integrated and pooled from populations as input to an effective dictionary learning and sparse coding algorithm, in order to identify common functional connectomes (CFC) and signature patterns, as well as their dynamic transition patterns. The computational framework was validated by benchmark stimulation data, and highly accurate results were obtained. By applying the framework on the datasets of 44 post-traumatic stress disorder (PTSD) patients and 51 healthy controls, it was found that there are 16 CFC patterns reproducible across healthy controls/PTSD patients, and two additional CFCs with altered connectivity patterns exist solely in PTSD subjects. These two signature CFCs can successfully differentiate 85% of PTSD patients, suggesting their potential use as biomarkers.

Index Terms— fMRI, DTI, Connectome

1. INTRODUCTION

Neuroscience research suggests that the function of any cortical area is not fixed, and each cortical area runs different “programs” according to the context and to the current perceptual requirements [1]. For instance, it has been observed that brain state change is a dynamical process of functional connectivity, even in resting state [2], and there exists “temporal functional modes” [3] or a switching between activation in default mode network and task positive networks [4]. Essentially, quantitative characterization of these time-dependent brain dynamics can elucidate fundamentally important temporal attributes of functional connections which cannot be revealed by traditional static functional connectivity analysis. Several methodologies have been developed in modeling the brain functional dynamics, including temporal ICA [3] and Bayesian network modeling [5]. While in this work, we

proposed a novel framework to capture the dynamics of functional connectomes, and to analyze the common functional connectomes (CFCs) by dictionary learning and sparse coding algorithms, and the framework pipeline is shown to the right of Fig. 1. We hypothesize that there exist quasi-stable brain states in R-fMRI data that can be quantitatively characterized, and the continuous functional status of the resting brain can be decomposed into a series of temporally concatenated representative CFCs. The whole framework is built based on the recently discovered and validated large set of consistent and correspondent cortical landmarks based on consistent DTI-derived fiber patterns [6], which offers a natural universal reference system across individuals and populations. We applied the framework to study PTSD (post-traumatic stress disorder) patient subjects along with health control subjects, and identified 16 common functional connectomes that could form the brain’s functional state space in resting state. Data from PTSD patients exhibited additional two altered connectomes, and it turned out that these two altered connectome patterns could be used as biomarkers for classifying PTSD patients with health control subjects.

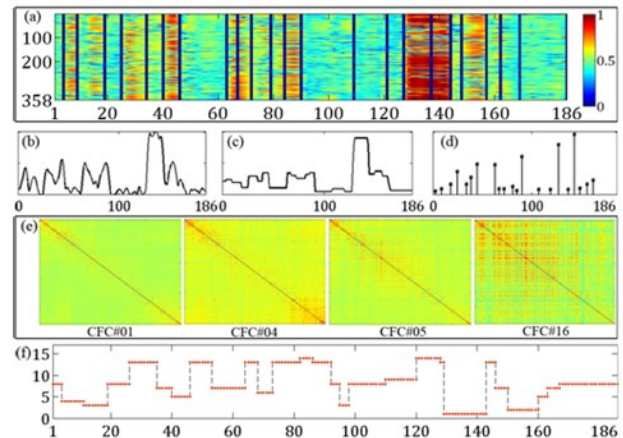


Fig. 1. Examples of results generated at each stage: (a) Functional connectome strength (FCS) of 358 ROIs from a randomly selected subject using Eq. (2). The dark blue lines highlight 23 automatically segmented brain states. (b) The global connectivity vector (GCV) derived from FCS. (c) The filtered GCV using Eq. (3). (d) State change points identified from the filtered GCV using Eq. (4). (e) 358*358 correlation matrix of four sample CFCs obtained from dictionary learning. (f) The projected brain dynamics. Each dot is the index of CFC that the FCS is projected to at each time window. The total number of CFCs is 16.

2. METHOD

2.1. Functional connectome and its dynamics

To investigate the dynamics of global whole-brain functional connectivity, defined as Functional Connectome (FC), we applied the sliding time window approach to measure a temporal FC_t at time point t out of all T time points, with the duration of window length l . Specifically, for each pair of temporal segments $X_{i,t}$ and $X_{j,t}$ from the fMRI time series of two ROIs (region of interest) i and j out of all I number of ROIs, we obtained the functional connectivity $R_{i,j,t}$ between them:

$$R_{i,j,t} = \text{corr}(X_{i,t}, X_{j,t}), X_{i,t} = \{fMRI_{i,t}, \dots, fMRI_{i,t+l}\} \quad (1)$$

FC_t characterizes the brain functional connectivity between all ROI pairs. For visualization and dimension reduction purposes, we defined the Functional Connectome Strength (FCS):

$$FCS_t = \sum_{j=1}^I R_{i,j,t}, FCS = \{FCS_1, FCS_2, \dots, FCS_{T-l}\} \quad (2)$$

FCS_t is the sum of functional correlation between each ROI and all the other ROIs at time t , which is an $I \times 1$ vector, and the i_{th} value in the vector is the strength of connectivity of the i_{th} ROI. Thus, FCS is the concatenation of FCS_t on all time points, and reflects the connectivity strength through the whole time course. An example visualization of FCS is shown in Fig. 1(a). As the example data contains 200 time points and the window length l was set to 14, the total number of windows is 186 in the example.

Furthermore, from Fig. 1(a) it could be seen that the brain functional connectome is in a state-like behavior, with abrupt changes in connectivity strength on the boundaries of states. Thus, in order to capture the state-like dynamics of FC and provide a data space for the subsequent dictionary learning and sparse coding, we designed an automatic approach to segment the temporal FC by performing filtering of the averaged FCS across all ROIs, defined as the Global Connectivity Vector, GCV. GCV is a $T \times 1$ vector that describes the global functional connectome strength dynamics, as shown in Fig. 1(b). It could be assumed that many adjacent values in GCV should be constant in each quasi-stable state, so we applied the L_1 -regularized fused-LASSO to model this piece-wise constant process, and the following energy function will be optimized:

$$E = \|GCV - x\|_2 + \lambda \|D(x)\|_1 + K \quad (3)$$

where D is the first-order difference function, and x is the filtered vector obtained from GCV with constant adjacent values regularized by λ . x would be the same as GCV with $\lambda=0$, and approaches a constant value K with $\lambda \rightarrow \infty$. An example filtered GCV is shown in Fig. 1(c). Then the local maximum of the first-order difference of the filtered GCV was identified as the change point for brain state change detection and segmentation:

$$y = \{D(x)_{1..w}, \dots, D(x)_{T-w..T-1}\}, P = \text{findmax}(y) \quad (4)$$

where y is the piece-wise partition of the first-order

difference of x . The length of each piece is w , a small value usually 1~3 time points long, as we are assuming no state change exists within this short interval. P are the indices of points in $D(x)$ which are the non-trivial local maximum in each piece. The change points are depicted in Fig. 1(d), and visualized as dark blue lines segmenting the FCS in Fig. 1(a). Derived from the results of Eqs. (3) and (4), we defined the brain states as a time period (t_1, t_2) identified by the automatic segmentation process in which the global functional connectivity strength remains quasi-stable, and the FCS of each brain state is defined as:

$$FCS_{state_i} = \sum_{t_1}^{t_2} FCS_t / (t_1 - t_2) \quad (5)$$

where the FCS of each brain state is defined as the averaged FCS of time points within this state bounded by (t_1, t_2), as we found that the brain state is jumping back and forth between limited numbers of similar connectome patterns, and such observation has been replicated in all of the cases of R-fMRI datasets we studied. It thus motivated us to propose the following Common Functional Connectome (CFC) modeling, based on the premise that 1) functional connectome pattern is stable in each brain state identified by the automatic method; 2) there exists large number of occurrence of such patterns, not only within each subject, but also across subjects, given that the 358 consistent cortical landmarks provides us a basis for the connectome pattern modeling at the group level.

2.2. Functional connectome modeling via dictionary learning and sparse coding

In this study, the recently developed Fisher Discrimination Dictionary Learning (FDDL) algorithm [7] based on Fisher discrimination criterion was tailored and optimized to model the common functional connectome. The basic idea of FDDL is to learn a structured dictionary D from a set of data A so that $A=DX$, where X is the coding coefficient. In the scope of this framework, A is the FCS_{state} obtained in Eq. (5), which describes functional connectome strength of brain states identified in Eq. (3) and (4) from multiple subjects. D contains certain numbers of sub-dictionary D_i corresponding to the potential classes of the data, under the constraint of maximizing the discriminative capacity of the dictionary. As the initialization, matrix A would firstly be pre-labeled by the component indices obtained by principle components. Then the energy function $J(D,X)$ would be optimized to obtain the learned dictionary, as well as the class labeling A_i of the data:

$$J_{(D,X)} = \text{argmin}_{(D,X)} \{r(A, D, X) + \lambda_1 \|X\|_1 + \lambda_2 f(X)\}$$

$$r(A, D, X) = \|A_i - DX_i\|_F^2 + \|A_i - D_i X_i^i\|_F^2 + \sum_{j=1, j \neq i}^k \|D_j X_j^i\|_F^2$$

$$f(X) = \text{tr}(\sum_{i=1}^c \sum_{x_k \in X_i} (x_k - \bar{X}_i)(x_k - \bar{X}_i)^T) - \text{tr}(\sum_{i=1}^c n_i (\bar{x}_i - \bar{X})(\bar{x}_i - \bar{X})^T) + \eta \|X\|_F^2 \quad (6)$$

$$\hat{A}_i = \operatorname{argmin}_{(i)} (\|A_i - DX_i\|^2) \quad (7)$$

The first term in the energy function, $r(A, D, X)$ is the constraint on discriminative fidelity, thus making the dictionary D able to code the data with minimum residual, while at the same time only using one sub-dictionary D_i , but not other sub-dictionaries. The second term is the sparse constraint, requiring the coding coefficient X be as sparse as possible, i.e., the total number of non-zero items in X should be minimized. The third term $f(X)$ is the constraint on the discriminative coefficient, which aims to minimize within-class scatter of X , and maximize cross-class scatter of X , according to Fisher discrimination criterion [13]. It has been shown in [7] that the energy function in Eq. (6) is convex and could be solved by iterative projection method. The learned dictionary D has the same dimension with matrix A , and contains sub-dictionaries corresponding to each class. Then the class labeling A_i would be rearranged so that the residual from coding could be minimized as in Eq. (7). The two energy functions in Eq. (6) and (7) would be optimized in turn iteratively until the solution converges or exceeds the max number of iteration.

To determine the optimal number of potential classes of the data (i.e. model order), the Bayesian Information Criterion (BIC) was used in the model framework, defined as:

$$BIC = n \ln(\hat{\sigma}_e^2) + k \ln(n) \quad (8)$$

where σ_e^2 is the estimation for error variance, and in this study it is defined as the summed variance of each entry in the matrix A within its corresponding class. n is the total number of entries in A , and k is the number of classes. There is a trade-off between the model order and the error variance, and the optimized number of states is determined a posteriori by finding the minimum BIC value from the model result (dictionary learned) by searching a range of model orders.

The final goal of this framework is to determine the CFCs of brain states, which could be defined from labeling of each class. As each entry in matrix A is corresponding to brain states previously identified, and it has been class-labeled during the learning, by averaging FC (correlation matrix) of brain states labeled to the same class, we could have one CFC (averaged correlation matrix) from each class as the representative connectome pattern of it (shown in Fig. 1(e)), based on the premise that similar connectome pattern is reoccurring within class. As another result of the framework, the encoded brain's functional dynamics could be obtained by projecting each time point in FCS by the learned dictionary to obtain its class label (index of CFCs). The projection could be done by applying the dictionary D to sparse-code the given matrix T , so long as T has the similar structure and type of information with A , while the total number of entries needs not to be the same. The sparse coding algorithm is based on the sparseness function developed in [8]:

$$\hat{X} = \operatorname{argmin}_{(X)} \|X\|_1, \text{ subject to } T = DX \quad (9)$$

where D is the dictionary learned in Eq. (6) and T is the new data. An example of the encoded brain functional dynamics is shown in Fig. 1(f).

3. RESULTS

3.1. Model application on PTSD data

In this study, post-traumatic stress disorder (PTSD) patients and healthy controls were recruited under IRB approvals. Multimodal DTI and R-fMRI datasets for 95 subjects including 51 adult normal controls and 44 adults PTSD patients were acquired on a 3T MRI scanner. Acquisition parameters for the scans were as follows. R-fMRI: 64×64 matrix, 4 mm slice thickness, 220 mm FOV, 30 slices, TR = 2s, total scan length = 400s; DTI: 256×256 matrix, 3 mm slice thickness, 240mm FOV, 50 slices, 15 DWI volumes, b-value = 1000. The 358 consistent cortical landmarks were obtained by structural connectivity inferred from DTI data, each of which was optimized to possess maximal group-wise consistency of DTI-derived fiber shape patterns. The detailed prediction approach was described in [6]. In this study, totally 2530 FCS_{state} were obtained, out of which 1032 were from 51 normal control and 1498 from 44 PTSD patient subjects. To test the model capability in identifying differences between PTSD patient and health control data, these FCS_{state} were divided into two separate groups for training and testing, and formed the 1265×358 training matrix A_1 and the 1265×358 testing matrix A_2 , where each entry in the matrix is a training/testing sample. That is, exactly half of the FCS_{state} from both PTSD patient and health control data was assigned to A_1 , and the other half was assigned to A_2 .

Then the dictionary as well as the data labeling and the corresponding CFCs was learned from training data A_1 as in Eqs. (6) and (7), where the model order (number of classes) was determined to be 18 by Eq. (8). As each entry in the matrix has been projected to its corresponding index of CFC (ordered by their frequency of occurrence), we could obtain the histograms of CFCs differentiated by PTSD patients and health controls according to the source of those entries, shown in Fig. 2. There is observable difference in the distribution between PTSD patient and health control datasets in CFC #13 and #14, where these two CFCs that only exist in patient data, but almost never occur in health controls. Furthermore, by sparse-coding T_2 using the dictionary learned, we found similar distributions of CFCs in the test data which was independent of the data used to learn the dictionary. Consistent with the CFC distribution in A_1 , there are almost no CFC #13 and #14 in the health control data in A_2 .

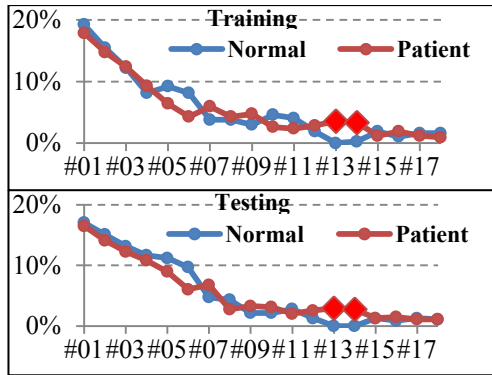


Figure 2: Histograms of CFCs in training and testing data. Labels on the x-axis are the indices of CFCs, values on the y-axis are their corresponding proportions in the data. Two signature CFCs that would be used for patient/control classification are highlighted by the red-colored diamonds.

Considering these two signature CFCs as the potential biomarkers for PTSD patient data, as visualized in Fig. 3, we projected all the time points in each subject into its corresponding CFC by the dictionary learned, and used the presence of CFC#13 and #14 for classifying the PTSD patient subjects from health controls: if a subject contains any time points projected to either of those two CFCs (out of 186 time points), it would be classified as PTSD patient subject. The classification result shows that over 85% of the PTSD patient subjects can be successfully classified (false negative rate < 15%), and only one health control subject was classified as PTSD patient (false positive rate < 2%).

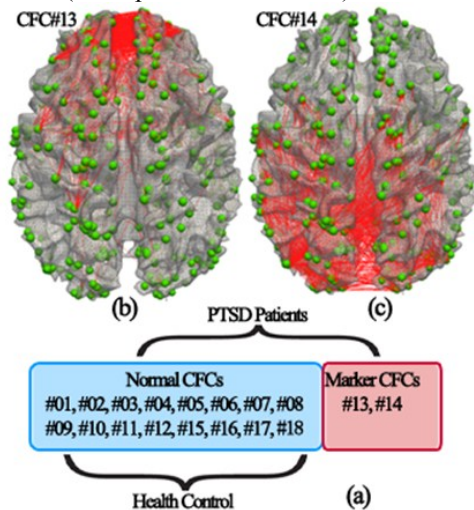


Figure 3: (a): Illustration of the CFC distribution in health control and PTSD patient subjects. (b)-(c): Visualization of CFC #13 and #14 on brain surface, where a global threshold ($=0.75$ for Pearson's correlation) was used to select the highest functional connectivities to demonstrate. ROIs are visualized as green spheres on the surface, and the functional connectivities between ROIs are visualized as red edges connecting those green spheres.

It is interesting that the two abnormal PTSD signature CFCs (#13 and #14) are characterized by the

hyper-connectivities in the frontal areas and the cingulate gyri, consistent with current neuroscience knowledge about PTSD that has been considered as an anxiety disorder associated with changes in extensive neural circuitries including frontal and limbic systems [9]. This result lends support to the validity and effectiveness of our connectomics signature discovery methods and results. The contribution of our work is that we quantitatively modeled and characterized the brain dysfunctions of PTSD by functional connectome patterns.

4. DISCUSSION AND CONCLUSION

In this study, we developed a novel framework for automatic discovery of common functional connectomes from resting-state functional fMRI across subjects and populations and for the automatic encoding of functional connectome dynamics. The framework utilized an effective global change point detection algorithm to identify quasi-stable brain states, then applied the Fisher Discrimination Dictionary Learning for capturing common functional connectomes in brain states, and finally used sparse coding for projecting the brain functional dynamics to the learned common functional connectomes. It was applied on the real R-fMRI data obtained from PTSD patient/healthy control subjects, and identified 16 common functional connectomes for all subjects and two altered signature connectomes for PTSD patient subjects. While the health controls and PTSD patient subjects share a large number of common functional connectomes, the two altered connectomes could potentially be used as biomarkers for differentiating PTSD patients.

5. REFERENCES

- [1] Gilbert CD & Sigman M (2007) Brain States: Top-Down Influences in Sensory Processing. *Neuron* 54(5):677-696.
- [2] Chang C & Glover GH (2010) Time-frequency dynamics of resting-state brain connectivity measured with fMRI. *NeuroImage* 50(1):81-98.
- [3] Smith SM, et al. (2012) Temporally-independent functional modes of spontaneous brain activity. *Proceedings of the National Academy of Sciences*.
- [4] Majeed W, et al. (2011) Spatiotemporal dynamics of low frequency BOLD fluctuations in rats and humans. *NeuroImage* 54(2):1140-1150.
- [5] Sun, J., et al., (2012) Inferring consistent functional interaction patterns from natural stimulus fMRI data. *NeuroImage* 61(4): p. 987-999.
- [6] Zhu D, Li K, Guo L, Jiang X, Zhang T, Zhang D, et al. (2012) DICCOL: Dense Individualized and Common Connectivity-Based Cortical Landmarks. *Cerebral Cortex*.
- [7] M. Yang LZ, X. Feng, D. Zhang (2011) Fisher Discrimination Dictionary Learning for Sparse Representation. *ICCV* 2011.
- [8] Wright J, Yang AY, Ganesh A, Sastry SS, & Ma Y (2009) Robust Face Recognition via Sparse Representation. *IEEE Trans. Pattern Anal. Mach. Intell.* 31(2):210-227.
- [9] Francati V, Vermetten E, Bremner JD. (2007) Functional neuroimaging studies in posttraumatic stress disorder: review of current methods and findings. *Depression and Anxiety.* 24(3).